Biomed Microdevices (2015) 17: 45
DOI 10.1007/s10544-015-9949-6

Tapered-slit membrane filters for high-throughput viable circulating tumor cell isolation

Yoon-Tae Kang · Il Doh · Young-Ho Cho

Published online: 20 March 2015

Abstract This paper presents tapered-slit membrane filters for high-throughput viable circulating tumor cell (CTC) isolation. The membrane filter with a 2D array of vertical tapered slits with a gap that is wide at the entrance and gradually decreases with depth, provide minimal cell stress and reduce 82.14 % of the stress generated in conventional straight-hole filters. We designed two types of tapered-slit filters, Filters 6 and 8, respectively, containing the tapered slits with outlet widths of 6 μm and 8 μm at a slit density of 34,445/cm^2 on the membrane. We fabricated the vertical slits with a tapered angle of 2 ° on a SU8 membrane by adjusting the UV expose dose and the air gap between the membrane and the photomask during lithography. In the experimental study, the proposed tapered-slit filter captured 89.87 % and 82.44 % of the cancer cells spiked in phosphate buffered saline (PBS) and diluted blood (blood: PBS=1:4), respectively, at a sample flow rate of 5 ml per hour, which is 33.3 times faster than previous lateral tapered-slit filters. We further verified the capability to culture on chip after capturing: 72.33 % of cells among the captured cells still remained viable after a 5-day culture. The proposed tapered-slit membrane filters verified high-throughput viable CTC isolation capability, thereby inaugurating further advanced CTC research for cancer diagnosis and prognosis.

Keywords Circulating tumor cells · Viable isolation · Tapered-slit filter

1 Introduction

The circulating tumor cells (CTCs), first discovered in the mid-19th century, refer to tumor cells that detach from the primary tumor site, circulate in the blood stream, and cause metastasis by forming secondary tumors. Current research on CTCs has focused on the clinical relevance to cancer, and that research recently verified that the number of captured CTCs from peripheral blood was relevant to the overall survival rate of patients (Cristofanilli et al. 2004). Furthermore, an elevated number of CTCs during cancer treatment indicated rapid progression of cancer for metastatic breast cancer patients in a clinical study of 177 patients (Hayes et al. 2006). These findings suggest that CTCs can be used as a biomarker for cancer diagnosis, prognosis and the measure of efficacy after cancer therapy.

Thus, various detection methods for capturing CTCs effectively using the CTC's properties have been investigated recently. Two main approaches, biochemical and physical methods, have been proposed for CTC isolation based on the distinctive characteristics of CTCs from normal blood cells. Biochemical methods use CTC specific antibody-antigen interactions, such as epithelial cell adhesion molecules (EpCAM), prostate-specific membrane antigen (PSMA), and synthesized aptamers depending on target tumor cells (Nagrath et al. 2007; Gleghorn et al. 2010; Xu et al. 2009). Though biochemical methods facilitate the high purity and low false-positive detection of CTCs, they show unstable capture efficiencies due to a heterogeneous expression level depending on the types of tumors. In addition, solely CTC isolation with viability after capture is limited because of irreversible antibody-antigen binding after biochemical treatment. Viable isolation of the CTC is essential for further long-term genetic and molecular analysis of the CTC. Physical methods that utilize the difference in size, density and electrical properties between CTCs and blood cells have been proposed in order to overcome those problems. Density gradient centrifuge, inertial microfluidics, dielectrophoresis manipulation, and filtration were proposed to make use of the physical properties of CTCs (Baker et al. 2003; Sim et al. 2011; Gascoyne et al. 2009; Zheng et al. 2007). In spite of relatively low specificity compared to biochemical

Y.-T. Kang · I. Doh · Y.-H. Cho (✉)
Department of Bio and Brain Engineering, Korea Advanced Institute of Science and Technology (KAIST), Daejeon, South Korea
e-mail: nanosys@kaist.ac.kr

methods, physical methods have shown stable capture efficiency regardless of the expression level of surface markers. Among them, filtration methods focusing on size of CTC, are widely used method for isolating CTC physically. However, previous microfilters having straight-holes commonly generated stress concentration at the entrance because diameter of entrance is normally small than diameter of target cells. Thus, cell rupture coming from concentrated tension stress on filter edge lowered the viability of CTC at high flow rate condition.

A double layer membrane with a straight-hole filter was proposed in order to support the captured cells and reduce the stress during continuous sample flow (Zheng et al. 2011), but this filter still had stress concentration at the entrance of the filter and required complex fabrication for making a two-membrane filter assembly.

We proposed a lateral tapered-slit array with a wide entrance and a gradually decreasing width to generate supporting force to cells and reduce the tension stress at the entrance (Doh et al. 2012). We verified the range of threshold pressure for selective CTC isolation from blood, considering both size and deformability by numerical analysis. The previous lateral tapered-slit array accomplished the viable cancer cell isolation based on both size and deformability of cancer cells. The throughput, however, was low (0.15 ml/h) because it was difficult to implement multiple slits in the lateral layout. In this work, we designed, fabricated, and verified the membrane filter having a vertical 2D tapered-slit array to achieve a high level of throughput and viability of cells. The increased number of tapered-slits achieved high-throughput sample processing, which took less than 10 min for 1 ml processing in a 1 cm^2 filter region, with capture efficiency of 89.87 %, and high viability after 5 days on the filter membrane, which is enough for further molecular study on CTCs.

2 Material and methods

2.1 Working principles

Figure 1 illustrates the schematic view of the presented tapered-slit filter. The tapered-slit filter consists of three layers: two chambers, top and bottom, for flow guidance and an SU8 filter for filtration of CTCs. The overall size of each layer was 16 mm×12 mm and the effective region for filtration was 10 mm×10 mm. Those three layers were assembled by a zig and used for the experiment.

The tapered-slit has advantages in cell isolation compared to a straight one; the wide entrance and decreasing width design eliminate the stress concentration on the edge by generating a supporting force. In addition, the tapered structure utilizes not only cell size but also deformability of the target cell to isolate it. Figure 1 shows the tapered-slit structure with a captured cell. The supporting force, P_{side}, compensates for the hydraulic force acting on a cell when the cell is passed through the tapered-slit structure. This design was previously verified to have a lower escape rate of target cells compared to the straight design (Doh et al. 2012). Thus, we optimized the tapered structure for high-throughput conditions with no critical cell damage. The following equation describes this relation (Hertz 1881):

$$P_{side}A_{side}\sin\ \theta = P_{in}A_{in} - P_{out}A_{out} \quad (1)$$

where P_{in}, P_{out}, P_{side}, A_{in}, A_{out}, A_{side}, and θ denote the inlet, outlet, side pressures on the cell, contact area for each pressure, and tapered angle, respectively. The 10 mm^2 area of the filter layer contains 34,445 tapered-slits, so the throughput was significantly increased compared to previous lateral tapered-slit filter with only 80 slits. In numerical estimation of cell behavior in a tapered slit, we verified the distinctive difference in threshold pressure (2.8 Pa for white blood cell, 11.3 Pa for CTC) in our tapered-slit design (θ: 2°, W_{out}: 6 μm, thickness: 100 μm) and found that CTCs could be selectively captured.

Thus we demonstrated that the presented tapered-slit filter is capable of achieving high throughput viable CTC isolation with a high probability of selective CTC isolation.

2.2 Design and analysis

The tapered-slit filter has 83×415 (=34,445) tapered-slits (Fig. 2). To determine the outlet width of the slit, W_{out}, we

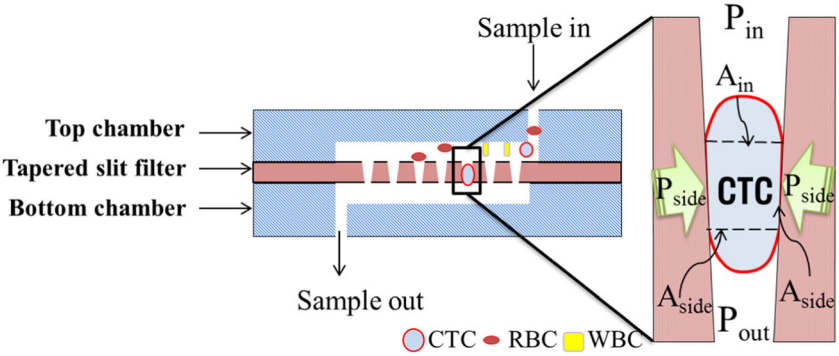

Fig. 1 Tapered-slit filter device for high-throughput viable isolation of circulating tumor cells, where *A* and *P* denote the area and pressure of each position

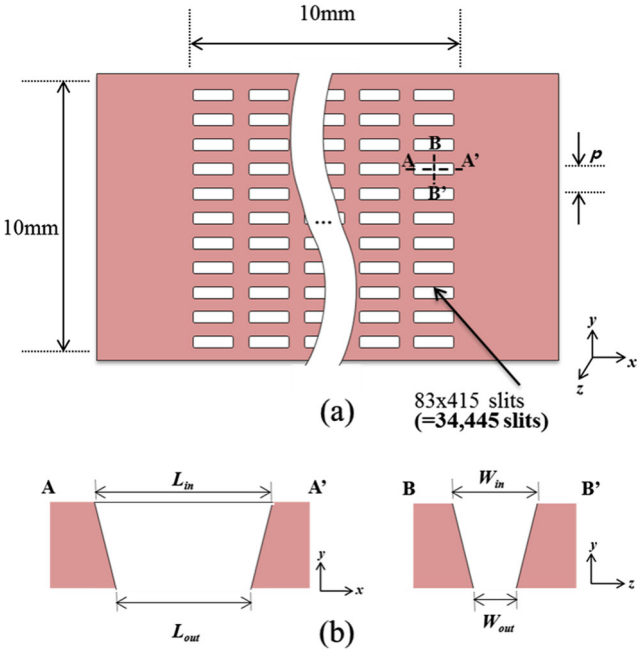

Fig. 2 Tapered-slit filter: (**a**) top view; (**b**) cross sectional views of the slit across A-A' (*left*) and B-B' (*right*)

need to consider the variations of blood cell size. The size of a CTC is bigger than that of white blood cells (7.5–8.5 μm) and red blood cells (6.2–7.9 μm) (Chien et al. 1970; Choi et al. 2007). The average size of the H358, which is a non-small-cell lung cancer (NSCLC) cell line, is 18.1 μm (Hosokawa et al. 2010). At the same time, in our previous work, the lateral tapered-slit array showed the highest capture efficiency at an outlet width of 6 μm. From these considerations, we designed two prototypes, Filter 6 and Filter 8, with outlet/inlet widths of 6/12 μm and 8/14 μm, respectively.

The material used for the tapered-slit filter was SU8, which is a well-known epoxy-based negative photoresist (PR) for patterning a high aspect ratio structure. In order to verify the mechanical suitability of the SU8 material as a filter, we performed a numerical estimation. According to the physical properties of SU8, we chose Young's modulus (E), Poisson's ratio (ν) and density (ρ) as 2 GPa, 0.22 and 1,200 kg/m^3, respectively. The dimensions of the SU8 filter used for modeling were 16 mm×12 mm. A 0.79 μm displacement was induced by applying 10 Pa pressure, which was identical to the flow rate of 13.25 ml/h used in this design. At the same time, the maximum strain, ε, was 1.5×10^{-5}, so that the change in slit dimensions was expected to be negligible. In other words, the SU8 material, which was first used in filter application here, could be an option as a filter for high flow rate conditions.

2.3 Fabrication procedure

The fabrication procedure of the tapered-slit filter, illustrated in Fig. 3, is divided into two parts: the tapered-slit filter and the top/bottom chambers.

We fabricated the SU8 tapered-slit filter by standard photolithography without any mold or multiple masks. The principles and mechanism of generating vertical sidewall were previously studied theoretically and experimentally (Jun Zhang et al. 2004). Here, the tapered-slit angle of 2° were formed from the adjusting UV exposure dose and the air gap between the substrate and the photomask during lithography; we experimentally observed that the decreased time and wider air gap between the substrate and photomask give rise to increase the width of tapered-slit and angle of sidewall.

For the disposable single use, we used polyethylene (PE) transparency film (CG3300, 3M) as a substrate. The PE film was well washed with acetone (99.5 %, OCI Co., Ltd.) twice, then 100 μm SU8-2050 PR (Microchem, Newton) was spin coated on the PE film substrate by a spin coater (K-359SD-1, KYOWARIKEN) in the following conditions: 500 rpm for 10 s and then 1400 rpm for 30 s. After overnight planarization, the SU8 was soft baked on a hotplate (WiseTherm HP20D, DAEHAN Scientific Co. Ltd.) and cooled down over an hour on the switched off hotplate. The UV exposure was carried out using an MA6 mask aligner (SUSS MicroTec.) at the conditions of a certain distance between the mask and substrate with an intensity of 260 mJ/cm^2. After the post exposure bake on the hotplate, the SU8 on the PE film was placed on the switched-off hotplate to prevent the SU8 from being curled

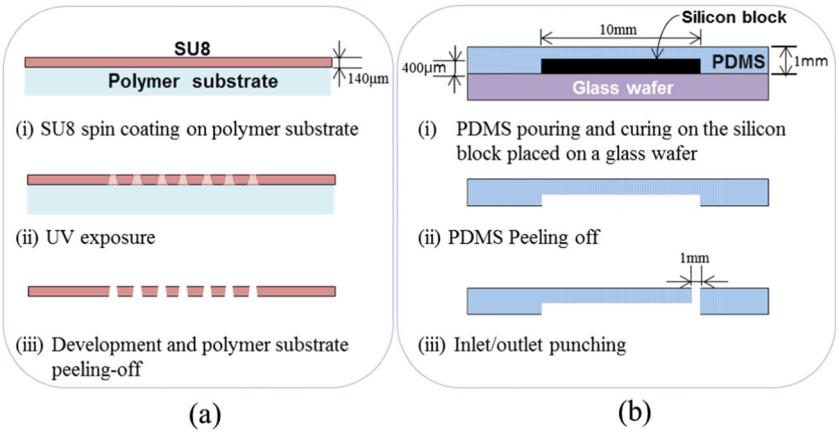

Fig. 3 Fabrication procedure: (**a**) tapered-slit filter; (**b**) top and bottom chambers

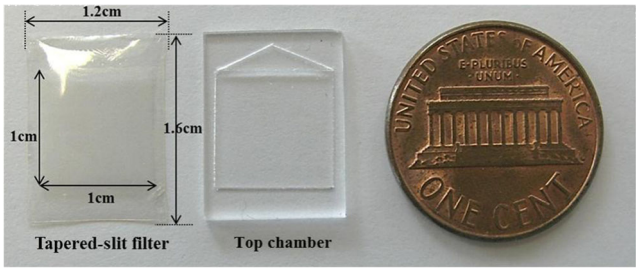

Fig. 4 Fabricated tapered-slit filter and chamber

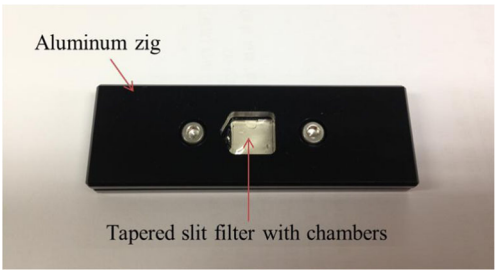

Fig. 6 Photograph of the tapered-slit filter device assembled with the aluminum zig

and developing micro-cracks. The development step was processed in a sonicator (Power Sonic 410, HWASHIN) with the SU8 developer (Microchem, Newton) for effective permeation into the high-aspect-ratio slits. During the first 2 min, short development was carried out for die detachment, and then an additional 5 min development was processed for effective slit formation after releasing each filter from the substrate. After rinsing with isopropyl alcohol (99.9 %, OCI Co., Ltd.), the released SU8 filter was hard baked with pressure on a hotplate to keep it from turning curly during the hard bake.

The top and bottom chambers were fabricated with standard soft lithography. We used 1 cm×1 cm diced 400 μm-thick silicon for the mold. A PDMS pre-polymer mixture (curing agent-to-PDMS ratio of 1:10, Sylgard 184, Dow Corning) was poured onto the mold and degassed in a vacuum chamber 10 times. After curing the PDMS on a 60 °C hotplate for 10 h, it was peeled from the mold, diced, and then punched to be ready for use.

Figure 4 is the fabricated tapered-slit filter device and Fig. 5 is an enlarged view of the tapered-slits on the filter. The overall dimensions of the tapered-slits were based on four fabrications with identical exposure doses and distances between the mask and substrate. Compared to the intended dimension of W_{out} of Filter 6, whose mask design was 6 μm, the fabricated dimension was narrower by nearly 1 μm. At the same time, the inlet width, W_{in}, became significantly wider than the top outlet width, W_{out}. The measured tapered angles of the vertical sidewall were 2.34 and 2.27° for Filters 6 and 8, respectively. A stable repeatability from SU8 UV-exposure fabrication for formation of the tapered-slits was observed from the regular fabricated dimension

The fabricated membrane and PDMS chambers were aligned and assembled without leakage using a zig. The zig had an open region for microscope observation and interconnection (Fig. 6).

2.4 Experiment

Figure 7 describes the experimental setup for tapered-slit filter characterization. A tube was interconnected between the syringe pump and outlet port after the assembly of the tapered-slit filter and chambers. We used a pipette tip to inject the sample at the inlet port to minimize cell loss in the process of tubing and easy sample washing. The tapered-slit filter was observed by a fluorescence microscope after sample flowing. We used a non-small-cell lung cancer (NSCLC) cell line, NCI-H358G, which was transfected with green fluorescent protein (GFP), in order to observe the cell in filter effectively.

We studied the capture efficiency of Filters 6 and 8 at a flow rate of 5 ml/h and 10 ml/h using the cancer cells spiked in PBS, and then measured the recovery rate and viability of the captured remaining cancer cells after recovery. Using spiked cells in blood, we also verified the capture efficiency depending on dilution ratios of blood at a flow rate of 5 ml/h. After that, we measured the recovery rate and the viability separately. The viability was measured using the overall captured cancer cells on filter without recovery.

The cells were cultured in cell culture media (RPMI, Gibco) and maintained in a CO_2 incubator (SANYO, MCO-18AIC) at a temperature of 37 °C and CO_2 level of 5 %. We suspended the cells in Dulbecco's phosphate buffered saline (PBS) at a concentration of 10^5 cells/ml. We enumerated the tumor cells with a fluorescent microscope after 1 μl of suspension was pipetted in a 96 well plate (PS-microplate, greiner bio-one). Then we diluted the suspension by using 20 μl of

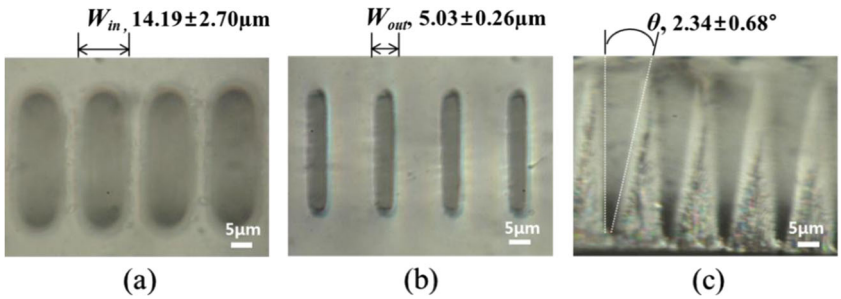

Fig. 5 Enlarged view of the tapered-slits on the filter (Filter 6): (**a**) top view; (**b**) bottom view; (**c**) cross sectional view

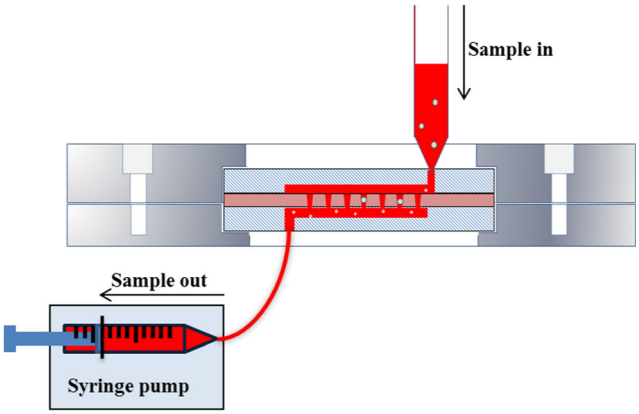

Fig. 7 Experimental setup for tapered-slit filter characterization

PBS in a well and spiked into PBS or diluted blood. In order to minimize the error for counting, we counted the number of tumor cells in well plate before-and-after aspiration three times, and obtained the precise number of spiked cells by subtracting remaining cell number in well plate from the initial suspended cells (Doh et al. 2012). A human blood sample was collected from healthy donors in an ethylenediaminetetraacetic acid (EDTA) tube (Vacuette, greiner bio-one) for anti-coagulation and used within 8 h after collection. The 1 ml diluted blood (1:4) was composed of 0.2 ml blood and 0.8 ml PBS solution.

We loaded the PBS with 1 % bovine serum albumin (BSA) solution 30 min before cell loading in the filter to avoid non-specific cell attachment to the PDMS chambers. Then the sample was injected to the inlet port and withdrawn by a syringe pump (Legato 180, KdS) from the outlet. The sample passed through the tapered filter at a flow rate of 5 or 10 ml/h. We added an additional 1 ml PBS after sample loading in order to wash out the remaining cells. We enumerated the captured cells in the filter 3 times carefully with a fluorescent microscope.

To recover the captured cells, we loaded the 3 ml of warmed (37 °C) RPMI media in a reverse direction at a flow rate of over 500 ml/h after measuring the capture efficiency to verify the possibility of recovery. The recovered sample fluid was carefully distributed in a 96-well plate (μCLEAR-PLATE, Greiner Bio-One), and then the cells in the fluid were enumerated for the measuring the recovery rate of captured cells. After tumor cell recovery, we counted the remaining cells showing fluorescence in the tapered-slit filter in order to count the initially viable remaining cells. We disassembled the filter from the zig and placed it in the petri dish containing fresh RPMI media. We cultured the remaining cells in the tapered-slit at a temperature of 37 °C and CO_2 level of 5 %, and the cells was closely observed daily. We injected additional fresh media into the petri dish every 2 days for appropriate culture conditions. After 5 days in the petri dish, we counted the viable cancer cells and measured the viability.

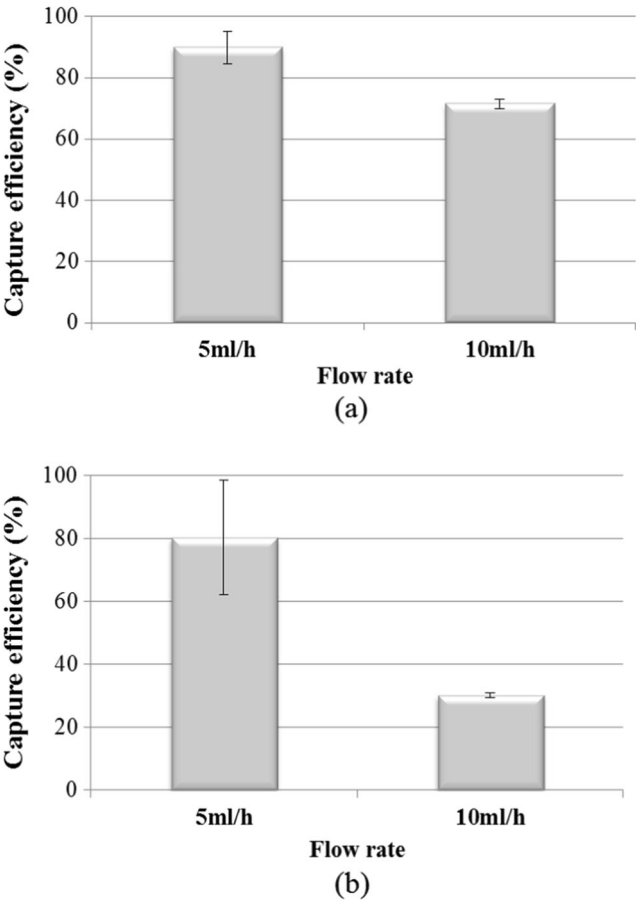

Fig. 8 Capture efficiency for the H358 cancer cells spiked in PBS depending on the sample flow rate supplied to different filters: (**a**) Filter 6; (**b**) Filter 8

3 Results and discussion

3.1 Cancer cells spiked in PBS

The capture efficiency of cancer cells (Fig. 8) was measured by counting the number of captured cells in the tapered-slit three times for accurate counting. At the same flow rate, as the

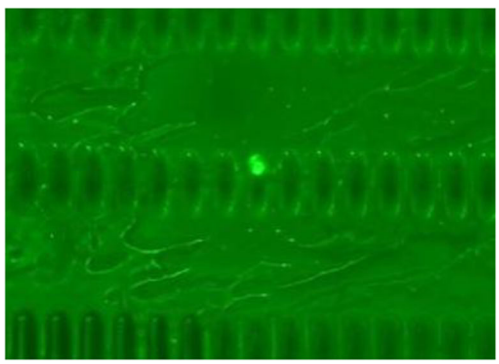

Fig. 9 The cancer cell cultured for 5 days after the cell capture at the tapered-slit filter (Filter 6) from the H358 cancer cell spiked in PBS

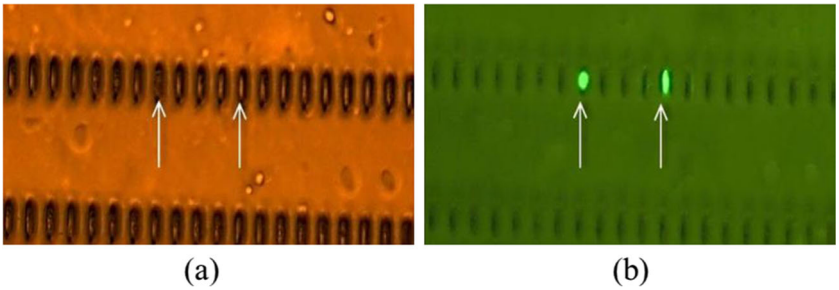

Fig. 10 The cancer cells captured by the tapered-slit filter (Filter 6) from the experiment using H358 cancer cells spiked in diluted blood (blood:PBS=1:2) at a flow rate of 5 ml/h: (**a**) bright field image; (**b**) fluorescent image

outlet width of the tapered-slit increased, the capture efficiency decreased in all cases. Filter 6 at a flow rate of 5 ml/h had 89.87 % capture efficiency while Filter 8 has a lower capture efficiency of 80.34 %.

We measured the capture efficiency of each of the two prototypes to ensure an optimal outlet width for a higher flow rate condition of 10 ml/h. Filter 6 had an overall efficiency decrease of 18.38 %, but Filter 8 suffered a dramatic efficiency decrease of 50.14 %. Since Filter 6 showed better capture efficiency at a flow rate of 5 ml/h and 10 ml/h; thus Filter 6 was verified as having the optimal design for CTC isolation at high flow-rate.

We recovered the captured tumor cells from the tapered-slit filter device by applying reverse flow into it. In this experiment, 59.14 % of the cells were recovered from the device for Filter 6 and 72.99 % of cells were recovered for Filter 8. Filter 8 had a higher recovery rate than Filter 6 in spite of showing lower capture efficiency than Filter 6. Since the dimension of Filter 8 is wider than Filter 6, the capturing ability of Filter 8 is lower and cell escape is easier than with Filter 6.

To verify the viability of captured cancer cells, we measured the viability of remaining captured cancer cells after 5 days of CTC capture and recovery. The cell expressing fluorescent protein showed fluorescence as long as they were alive; survival and growth of the GFP cell line can be assessed by their fluorescence (Bichsel et al. 2012). Figure 9 denotes the captured cells, still showing fluorescent after 5 days, which means that cells can be cultured in an SU8 environment. We verified that 70.24 % of the cells were viable from observation of two cases. The SU8 was shown to be biocompatible previously with neuron culture on SU8 (Choi et al. 2003). Recently, 2D microelectrode arrays made of SU8 were used for neuron culture; thus, our findings also support those results about biocompatibility of SU8.

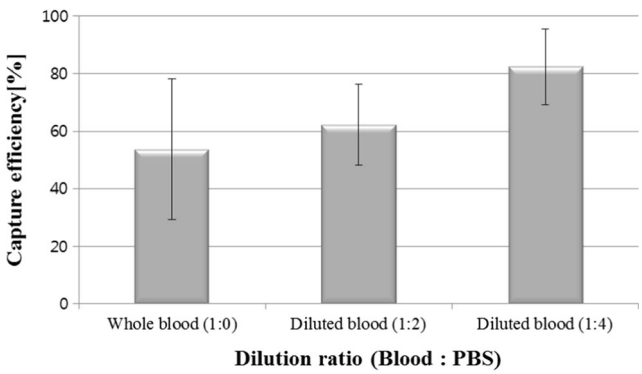

Fig. 11 Capture efficiency of the Filter 6 from the experiment using H358 cancer cells spiked in blood with various dilution ratios at a flow rate of 5 ml/h

3.2 Cancer cells spiked in blood

We verified that Filter 6 and 5 ml/h are the optimal conditions for CTC isolation from cancer cells spiked in PBS, so this condition was adopted for cancer cells spiked in blood. Figure 10 shows the cancer cells captured by Filter 6 using spiked cancer cells in diluted blood under bright field and fluorescence.

The capture efficiencies at various dilution ratios were verified to find an effective dilution ratio and identify the effect of the viscosity of blood. The capture efficiency decreased as the blood became less diluted (Fig. 11). One ml of whole blood was found to be processed without significant clogging of red blood cells at a flow rate of 5 ml/h; however, the capture efficiency using whole blood decreased by 28.63 % compared to diluted blood (blood:PBS=1:4). Thus, we used a dilution ratio of 1:4 for the experiment of cancer cells spiked in blood. At the same time, the overall time required for processing 1 ml of blood sample was about 12 min. It is highly improved than previous lateral tapered-slit filter (400 min/ml) (Doh et al. 2012) in terms of throughput. Previous membrane filter devices having straight hole processed the blood sample within 5 min. (1–5 min/ml, 3–5 min/ml) (Hosokawa et al. 2010;

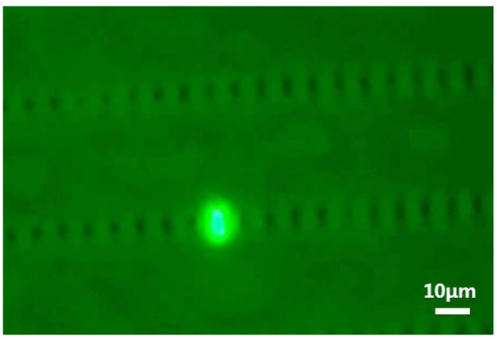

Fig. 12 The fluorescence image of the captured H358 cancer cell: the cell captured by the tapered-slit filter (Filter 6) and cultured for 5 days

Zheng et al. 2011). However, the device processing time is depends on hole density, device overall size, and dilution ratio of the blood sample. Thus, the throughput considering those factors is needed for the direct comparisons.

In this experiment, 82.44 % of the tumor cells were captured on the slit. Compared to the PBS spiking test at the same conditions, capture efficiency decreased by 7.43 %. Further design optimization, such as slit density improvement and pretreatment of RBC, would bring out better capture efficiency and throughput for CTC capture.

The proposed filter demonstrated a 36.04 % recovery rate from Filter 6. During recovery process, blood cells, which were remained and adsorbed non-specifically in tubing and SU8 tapered-slit filter, were also collected. We thought the uncounted CTCs were hidden by blood cells, and further surface treatment eliminating non-specific adsorption of blood cells would improve the recovery rate.

In order to identify more comprehensive CTC culture on SU8 filter, we demonstrated the culturing experiments separately without recovery of captured cancer cells from the filter. The culture conditions were identical to the ones for the CTC spiked in PBS. Figure 12 shows the captured CTCs were viable after 5 days from the CTC capturing experiments using diluted blood. We observed 72.33 % of viability of the CTCs. From this finding, we could see that CTCs can be cultured 5 days in an SU8 environment. Researches on the optimal condition for long-term CTC culture on SU8 and its proliferation are needed for further analysis of captured CTCs.

4 Conclusion

We proposed a tapered-slit filter for high-throughput viable CTC isolation. This membrane filter with tapered-slits accomplished capture efficiency of 89.87 % and 82.44 % in an experiment using cancer cells spiked in PBS and diluted blood (1:4), respectively, with theoretically minimal cell stress reduced to 18 % of the stress generated in conventional straight-hole filters. The time required for processing a sample was 33.3 times shorter than previous lateral tapered-slit filters, which is comparable to conventional straight-hole filter. Moreover, the captured CTCs cultured on the SU8 filter were viable after 5 days the experiment, which enables long-term molecular analysis of CTCs. Thus, tapered-slit filters have potential to be adopted in a viable CTC isolation kit or medical equipment using CTCs for cancer diagnosis and prognosis.

Acknowledgments This research was supported by the Converging Research Center Program funded by the Ministry of Science, ICT and Future Planning (Project No. 2014048778)

References

M. Cristofanilli, G.T. Budd, M.J. Ellis, A. Stopeck, J. Matera, M.C. Miller, J.M. Reuben, G.V. Doyle, W.J. Allard, L.W.M.M. Terstappen, D.F. Hayer, New Engl. J. Med. **351**, 781–791 (2004)

D.F. Hayes, M. Cristofanilli, G.T. Budd, M.J. Ellis, A. Stopeck, M.C. Miller, J. Matera, W.J. Allard, G.V. Doyle, L.W.W.M. Terstappen, Clin. Cancer Res. **12**, 4218–4224 (2006)

S. Nagrath, L.V. Sequist, S. Maheswaran, D.W. Bell, D. Irimia, L. Ulkus, M. Smith, E.L. Kwak, S. Digumarthy, A. Muzikansky, P. Ryan, U. Balis, R.G. Tompkins, D.A. Haber, M. Toner, Nature **450**, 1235–1239 (2007)

J.P. Gleghorn, E.D. Pratt, D. Denning, H. Liu, N.H. Bander, S.T. Tagawa, D.M. Nanus, P.A. Giannakakou, B.J. Kirby, Lab Chip **10**, 27–29 (2010)

Y. Xu, J.A. Philips, J. Yan, Q. Li, Z.H. Fan, W. Tan, Anal. Chem. **81**, 7436–7442 (2009)

M.K. Baker, K. Mikhitarian, W. Osta, K. Callahan, R. Hoda, F. Brescia, R. Kneuper-Hall, M. Mitas, D.J. Cole, W.E. Gillanders, Clin. Cancer Res. **9**, 4865–4871 (2003)

T.S. Sim, K. Kwon, J.C. Park, J.G. Lee, H.I. Jung, Lab Chip **11**, 93–99 (2011)

P.R.C. Gascoyne, J. Noshari, T.J. Anderson, F.F. Becker, Electrophoresis **30**, 1388–1398 (2009)

S. Zheng, H. Lin, J.Q. Liu, M. Balic, R. Datar, R.J. Cote, Y.C. Tai, J. Chromatogr. A **1162**, 154–161 (2007)

S. Zheng, H.K. Lin, B. Lu, A. Williams, R. Datar, R.J. Cote, Y.C. Tai, Biomed. Microdevices **13**, 203–213 (2011)

I. Doh, H.I. Yoo, Y.H. Cho, J. Lee, H.K. Kim, Appl. Phys. Lett. **101**, 4 (2012)

H. Hertz, J. Math. Crelle's J. **92**, 19 (1881)

S. Chien, S. Usami, R.J. Dellenback, M.I. Gregersen, Am. J. Physiol. **219**, 136–142 (1970)

S. Choi, S. Song, C. Choi, J.K. Park, Lab Chip **7**, 1532–1538 (2007)

M. Hosokawa, T. Hayata, Y. Fukuda, A. Arakaki, T. Yoshino, T. Tanaka, T. Matsunaga, Anal. Chem. **82**, 6629–6635 (2010)

J. Zhang, M.B. Chan-Park, S.R. Conner, Lab Chip **4**, 646–653 (2004)

C.A. Bichsel, S. Gobaa, S. Kobel, C. Secondini, G.N. Thalmann, M.G. Cecchini, M.P. Lutolf, Lab Chip **12**, 2313–2316 (2012)

Y. Choi, R. Powers, V. Vemekar, A. B. Frazier, M. Laplaca, and M. G. Allen, in High aspect ratio SU-8 structure for 3D culturing of neurons: Proceeding of ASME International Mechanical Engineering Congress and RD&D Expo, Washington, D.C., USA, 15–21 November 2003, pp 1–4